

Electrodeposition of patterned CdSe nanocrystal films using thermally charged nanocrystals

Mohammad A. Islam and Irving P. Herman^{a)}

Department of Applied Physics and Applied Mathematics, and the Materials Research Science and Engineering Center, Columbia University, New York, New York 10027

(Received 14 December 2001; accepted for publication 1 April 2002)

A dc electric field is used to attract charged CdSe nanocrystals in hexane to rapidly form very smooth, robust, large-area, several micron-thick films of equal thickness on both electrodes. This deposition on both electrodes implies there are both positively and negatively thermally charged dots, unlike conventional electrophoretic deposition. With patterned electrodes, controllable and locally selective assembly is achieved. © 2002 American Institute of Physics.

[DOI: 10.1063/1.1480878]

Use of nanocrystals as the building blocks of complex structures requires improved ways of forming films and complex patterned structures from these quantum dots. While there are ways of forming small ordered monolayers¹ and crystals² of dots, there is no satisfactory method to deposit large areas of uniform multimonolayer films. Dry casting, i.e., the evaporation of dots in solution, and spin coating result in films that are typically not uniform and by nature unpatterned; patterned films may be needed in device applications. We report a way to rapidly form large areas of very smooth, robust, several micron-thick films of dots that can be either unpatterned or selectively patterned.

In solution, CdSe dots appear to have a permanent dipole moment and a fraction of them are thermally charged.^{3,4} A uniform dc electric field is used to attract those charged CdSe nanoparticles to form films of controllable and equal thickness on both electrodes, suggesting equal densities of positively and negatively charged dots. These charged particles can be locally and selectively transported to the surface for spatially controllable assembly using patterned electrodes. This method differs from the electrophoretic deposition of an ordered monolayer of micron-size latex spheres and smaller particles,⁵⁻⁷ direct electrochemical formation of nanoparticles,⁸ and more conventional electrophoretic deposition of particles, which is usually in polar solvents with particles without organic ligand capping and where films are formed on one electrode with bulklike density.^{9,10}

CdSe nanocrystals were prepared according to the methods of Ref. 11, with trioctylphosphine (TOPO) capping ligands. Solutions of these dots (usually ~ 3.2 nm diameter) with densities 10^{15} – 10^{16} /cc ($\sim 4 \times 10^{-5}$ – 4×10^{-4} volume fractions) were prepared with hexane. Two electrodes, usually rectangular sections of Si wafers coated over 0.8×1.4 cm by 10 nm Ti and then ~ 150 nm Au, separated by ~ 1.4 mm, were submerged in a beaker with this solution. dc voltages up to 1000 V were applied across the electrodes at room temperature in the dark, with solvent added as needed to counter any evaporation. dc current was monitored during

runs, and the deposits on the electrodes were examined afterward.

The initial current between the electrodes was 60–70 nA [54 – 63 nA/cm² for 318 V (2.2×10^5 V/m), 1.0×10^{15} dots/cc], and linearly proportional to both voltage V and dot density n ; it decreased from 70 to ~ 25 nA in 45 min. Without dots, the current was $\sim 100\times$ smaller with the hexane solvent only and $20\times$ smaller with TOPO dissolved in hexane (with TOPO mass half that of the usual dot mass).

Uniform, apparently identical films formed on both unpatterned electrodes. No deposit was formed without the voltage. Visible microscopy, scanning electron microscopy (SEM), profilometry, and atomic force microscopy showed that both films were very smooth, with ~ 2 – 4 dot roughness for a ~ 1000 dot thick film. The initial deposition rate was $\sim (0.010$ nm/s) V (in volts) n (in 1.0×10^{15} dots/cc), per electrode. After long runs (45 min, 318 V, 1.0×10^{15} dots/cc), 3.4 μ m thick films were deposited (as shown in Fig. 1)—most of which formed within 20 min. After drying, these films did not dissolve in hexane (as do those formed by dry casting), even when voltage of either polarity was applied across it to a bare Au electrode. Transmission electron microscopy of these quickly grown thick films did not show ordered dots.

Photoluminescence (PL) of these films (Fig. 2) reveals one sharp peak near 567 nm (exciton emission) and two smaller peaks at 654 and 745 nm (possibly due to defects). In dot solutions, there is a 541 nm absorption and 560 nm PL peak. The strong 567 nm PL peak (stable for at least two

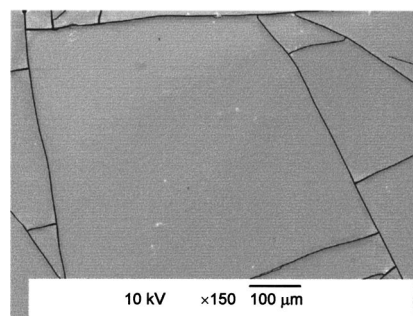


FIG. 1. SEM of 3.4 μ m thick electrodeposited film.

^{a)} Author to whom all correspondence should be addressed; electronic mail: iphl@columbia.edu

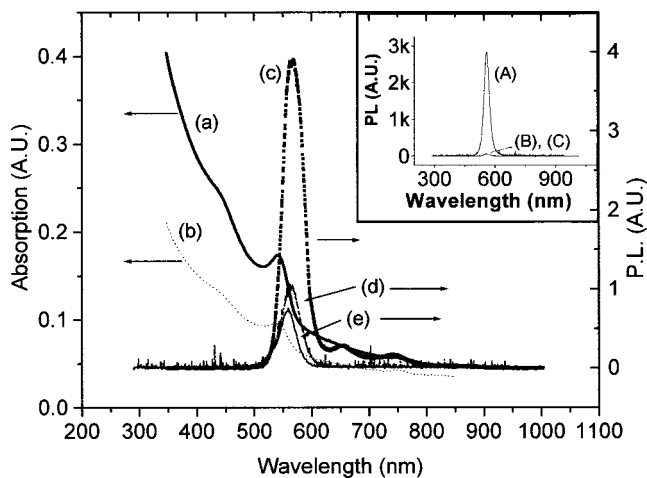


FIG. 2. Absorption of dot solution (a) before and (b) after electrodeposition, and PL of the (c) 3.4 μm thick electrodeposited film, (d) dry cast film, and (e) dot solution. The inset shows PL from the patterned dot film (A), and from regions with no Au film (B) and unconnected Au films (C).

months) shows the films consist of CdSe dots that are not greatly changed from solution (same radius, capping remains, etc). The 27 meV red PL shift in the film is due to fast interdot radiative transfer between nearby dots to larger, lower-band-gap dots;¹² this is also seen in the weaker PL from dry cast films.

The initial current decreased from 70 to 55 nA when hexane was replaced by octane (3.2 nm dots). The current per unit dot density was $\sim 3\times$ larger for larger 4.1 nm diameter dots in hexane, and the deposition rate per unit dot density was a bit larger (thickness rate by 2.2 \times , monolayer rate by 1.8 \times , dot rate by 1.2 \times). With lower conductivity

electrodes (Si with native oxide instead of Au) or impurities in the dot solution (added TOPO or remnants from incomplete cleaning of the synthesized dots), the current was unchanged, but fewer dots were deposited and the film quality was poor (patchy, clumpy, and sometimes on one electrode).

Figure 3 shows deposition on electrodes with Au/Ti films patterned on 0.2 μm thick silicon dioxide. Deposition, with micron-level lateral resolution, occurs selectively only on top of the Au connected to the electrode shown in the SEMs (regions A); there was very little or no deposition on the bare oxide (B) and patterned gold regions not electrically connected to the electrode (C), as confirmed by profilometry in Fig. 3 and PL (weaker by 50 \times) in the inset to Fig. 2.

Films sometimes showed cracking after drying, which is typical when solvent evaporates during the drying of films.^{13,14} In Fig. 1, the cracks are $\sim 5\ \mu\text{m}$ wide and occupy $4\% \pm 2\%$ of the film area, with the lateral dimensions of the islands often exceeding many hundreds of μm in this film. Cracking was not seen in the patterned dot regions in Fig. 3 and the unpatterned counter electrode film ($\sim 0.8\ \mu\text{m}$ thick), and in other $<0.8\ \mu\text{m}$ thick films.

The loss of dots in the solution due to deposition was tracked using absorption, calibrated by the mass of the dry dots (with TOPO capping), and compared to the number of dots deposited. The deposited number is $0.74At/(4\pi R^3/3)$, where A is the total electrode area, t is the film thickness (same for each electrode), R is the effective radius of each dot including capping ligand (2.15 nm for 3.2 nm diameter dots²) and the 0.74 assumes face-centered-cubic packing; this was smaller by $\sim 24\%$. This difference is attributable to systematic errors in the absorption cross section and particle

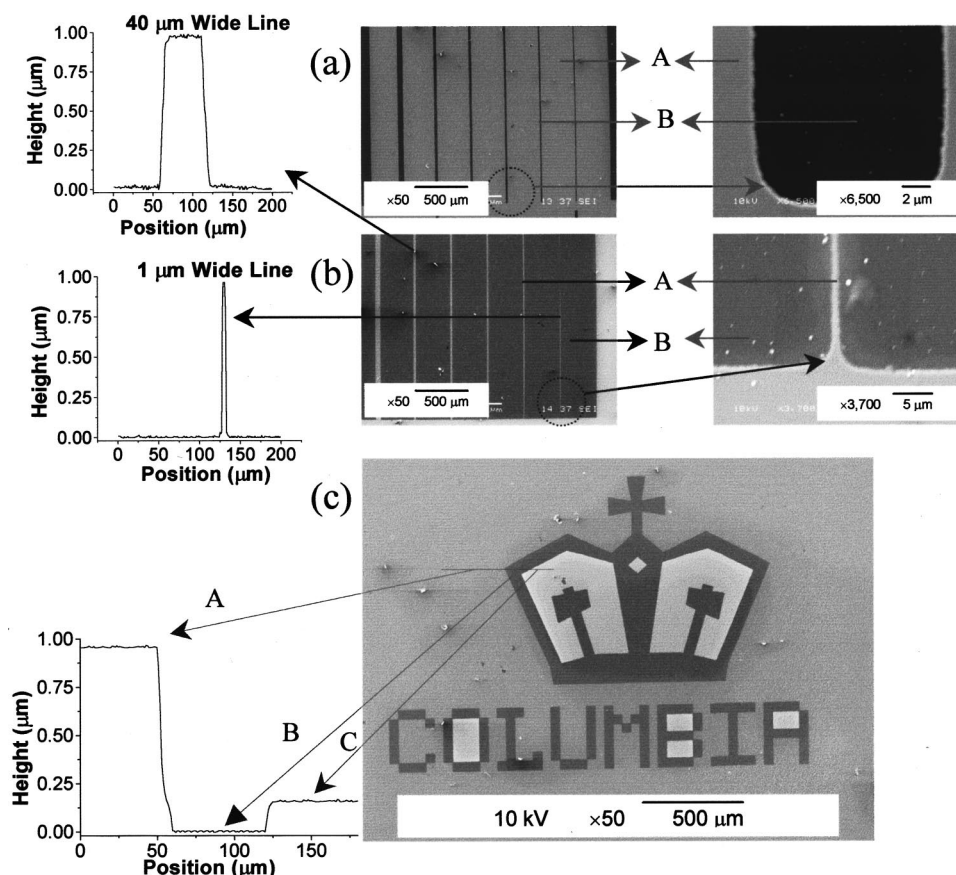


FIG. 3. Selective electrodeposition of 0.8 μm thick films on top of patterned Au films—connected to the electrode—atop 0.2 μm thick silicon dioxide (regions A), with very little or no deposition on the bare oxide (B) and patterned gold regions not electrically connected to the electrode (C). The SEMs in (a) and (b) show this for thin gold spacers and lines, respectively, with expanded SEM views to the right-hand side and profilometry traces to the left-hand side. The profilometry scan for the SEM in (c), shows the thickness for regions (A) (0.8 μm thick dot film atop 0.15 μm thick Au film), (B), and (C) (unconnected 0.15 μm thick Au film). The calibration bar is 500 μm in the left-hand side SEMs, and 2 μm (a) and 5 μm (b) in the expanded SEMs. See also the inset to Fig. 2.

diameter, less than close-packing densities, and film cracking. Using either method, more dots were deposited than elementary charges collected. For 3.2 nm dots, the ratio of dots deposited to charges collected was $\sim 44, 30, 28, 21,$ and 13 averaged over 10 min, 20 min, 30 min, 45 min, and 90 min runs, respectively, which shows that the deposited rate decreased even faster than the current. The ratio was ~ 6.6 for 4.1 nm dots (45 min).

The initial conductivity of the 3.2 nm/hexane solution was $\sigma = 2.75 \times 10^{-9}$ ohm m. For a solution of density n_{charged} dots with charge e and hydrodynamic radius R , the Nernst-Einstein equation is $\sigma = n_{\text{charged}} e^2 / 6\pi \eta R$, where η is the viscosity coefficient (3.26×10^{-4} N s/m²). If there are positive and negative dots with densities n_+ and n_- , then $n_{\text{charged}} = n_+ + n_-$. If there are no other counter ions, then the equal film thickness on both electrodes suggests $n_+ = n_- = n_{\text{charged}}/2$. Taking e as the elementary charge, $n_{\text{charged}} = 1.4 \times 10^{12}/\text{cc}$, or 0.14% of the nanocrystals are charged, half positively and half negatively. If a larger charge per dot were assumed, n_{charged} would be smaller and the ratio of the number of deposited dots per charged dot would be larger. If much of the voltage drop were near the electrodes,⁹ the conductivity in the bulk solution would be much larger than calculated here. This would make n_+ and n_- larger, but not change the ratio of collected dots to charge. Changing the solvent from hexane to octane decreased the current consistent with the increase in η from 3.26 to 5.48×10^{-4} N s/m². For 4.1 nm diameter CdSe dots in hexane, 0.55% of dots are charged. The energy needed to put a charge on the core of these 3.2 nm dots is estimated to be ~ 0.15 eV (from midgap states of one dot to another).⁴ The observed fraction of charged dots is consistent with that estimated from the Boltzmann factor.

For the 3.2 nm dots, in 45 min $\sim 120\times$ as many dots were deposited as were initially between the electrodes. If 0.14% of the dots were charged, $360\times$ all initially charged dots and $\sim 90\,000\times$ of initially charged dots between the electrodes were deposited. This suggests that charge equilibration and diffusion between the reservoir and electrode volume occur in < 20 s, so the decrease in current with time is most likely due to the depletion of dots in solution (and possibly the varying conductivity of the deposited film).

Electric-field assisted deposition can be dominated by the bulk electric field transport of charged species, i.e., electrophoresis, or interfacial electrochemistry due to charge transfer at the electrodes. Most electrophoretic studies of the forming layers of particles (charged latex,^{5,6} and gold^{6,7}) have been conducted in aqueous solutions in which the solvent played a major role in the effective particle charge and charge screening, the applied voltages were much lower, and deposition was on only one electrode. The hexane solvent used here is very "inert" in forming anions and cations, polarizing the dissolved medium, and screening.¹⁵ Interdot charge transfer is quite possible here, though some role of very low-concentration electrolytes can not be discounted.

The electric field produced by a monolayer of singly charged CdSe/TOPO dots is 5×10^8 V/m (ignoring image charges), which is $\sim 1000\times$ the maximum applied fields,

$\sim 7 \times 10^5$ V/m, so charge transfer through the thick films and to the electrode must be fast. The conductivity of dried CdSe dots films is very low.^{16,17} However, the conductivity of dot solutions increasing rapidly for dot volume fractions exceeding 0.1 suggests that the solvent permeating these films in solution provides a sufficient conductivity path.⁴

The faster decrease of the deposition rate than current suggests that deposition is hindered on thicker films, which is consistent with the observed sensitivity of deposition to the electrode material. The much larger number of dots deposited than charges collected could suggest: (1) Each charged dot transfers its charge to the electrode and is deposited. The other dots could be collected by hydrodynamic flows or gradients caused by the transport of charged dots, but this may be inconsistent with micron-resolution patterning. (2) Each charged dot is deposited, but only a fraction of the charges are transferred to the electrodes. This is counter to impurities decreasing the deposition rate, but not the current. (3) The large conductivity of dot solutions for large dot volume fractions³ may mean faster interdot charge transfer near the electrodes due to the higher densities, which may lead to a high flux in steady state with the same current flow. (4) The nanoscale roughness of the surface could produce electric-field gradients that attract the dipolar uncharged dots.

This deposition method should be applicable to many or all nanocrystals and nanorods, since thermal charging appears to be very common, and to mixtures of them.^{3,4} Simultaneous deposition of patterned films on both electrodes is feasible and the film thickness can be separately controlled for different electrodes on a substrate. One would expect ordered layers would form for slower deposition rates and very thin films.

The authors thank Alan West, Louis Brus, Luc Frechette, and Jon Spanier for helpful discussions. This work was supported primarily by the MRSEC Program of the National Science Foundation under Award No. DMR-9809687.

¹X. M. Lin, H. M. Jaeger, C. M. Sorensen, and K. J. Klabunde, *J. Phys. Chem. B* **105**, 3353 (2001).

²C. B. Murray, Ph.D. thesis, MIT, 1995.

³S. A. Blanton, R. L. Leheny, M. A. Hines, and P. Guyot-Sionnest, *Phys. Rev. Lett.* **79**, 865 (1997).

⁴M. Shim and P. Guyot-Sionnest, *J. Chem. Phys.* **111**, 6955 (1999).

⁵M. Trau, D. A. Saville, and I. A. Aksay, *Science* **272**, 706 (1996).

⁶S. Yeh, M. Seul, and B. I. Shraiman, *Nature (London)* **386**, 57 (1997).

⁷M. Giersig and P. Mulvaney, *Langmuir* **9**, 3409 (1993).

⁸Y. Zhang, G. Hodes, I. Rubinstein, E. Grünbaum, R. R. Nayak, and J. L. Hutchison, *Adv. Mater.* **11**, 1437 (1999).

⁹P. Sarkar and P. S. Nicholson, *J. Am. Ceram. Soc.* **79**, 1987 (1996).

¹⁰O. O. Van der Biest and L. J. Vandeperre, *Annu. Rev. Mater. Sci.* **29**, 327 (1999).

¹¹C. B. Murray, D. J. Norris, and M. G. Bawendi, *J. Am. Chem. Soc.* **115**, 8706 (1993).

¹²C. R. Kagan, C. B. Murray, M. Nirmal, and M. G. Bawendi, *Phys. Rev. Lett.* **76**, 3043 (1996).

¹³S. Kitsunezaki, *Phys. Rev. E* **60**, 6449 (1999).

¹⁴A. T. Skjeltorp and P. Meakin, *Nature (London)* **335**, 424 (1988).

¹⁵D. Aurbach and I. Weissman, in *Nonaqueous Electrochemistry*, edited by D. Aurbach, (Marcel Dekker, New York, 1999), Chap. 1.

¹⁶C. A. Leatherdale, C. R. Kagan, N. Y. Morgan, S. A. Empedocles, M. A. Kastner, and M. G. Bawendi, *Phys. Rev. B* **62**, 2669 (2000).

¹⁷D. S. Ginger and N. C. Greenham, *J. Appl. Phys.* **87**, 1361 (2000).